



## Lattice Gauge Theory Spectrum for Broken $SU(4)$

HUGH BERGKNOFF

Fermi National Accelerator Laboratory, Batavia, Illinois 60510

### ABSTRACT

The lattice gauge theory's hamiltonian formulation is reviewed. We present a theory involving 4 quarks; a massless  $SU(2)$  doublet (u and d) and in addition, two massive quarks (c and s). Calculations of the theory's strong coupling expansion are described, and mass ratios for 6 particles ( $\psi, \phi, \Lambda, \Lambda_c, F, F^*$ ) are constructed. The results agree with the physical spectrum to 12% and exhibit sensible dependences on the input masses for the s and c quarks.



## I. INTRODUCTION

Quantum chromodynamics<sup>1</sup> is a presently popular model for strong interaction physics. The theory is asymptotically free<sup>2</sup> and conjectured to involve strong coupling at large distances. The lattice version of the theory<sup>3,4</sup> is a gauge invariant regularization which exhibits confinement in the strong coupling regime. In the lattice theory, strong coupling expansions may be constructed.

The hamiltonian form of the lattice theories has been used extensively in the investigation of model field theories.<sup>5,6</sup> Strong coupling expansions for the lattice Schwinger model have been compiled to 8th order.<sup>5</sup> The results of this computation agree well with known quantities available from the exactly solvable continuum theory. Also, the lattice hamiltonian method has been successfully applied to the SU(N) Thirring model.<sup>6</sup>

In four dimensions, the spectrum of the pure SU(3) gauge theory has been explored,<sup>7</sup> and so has the hadron spectrum of a theory of gluons interacting with an SU(2) doublet of massless quarks.<sup>8</sup> In this paper, I shall report the results of strong coupling expansions for a theory of broken SU(4); a theory incorporating strange and charmed quarks in addition to the massless isodoublet of "u" and "d" quarks.

Strong coupling expansions for 6 particles are computed. They are the  $\psi$  ( $c\bar{c}$  vector),  $\phi$  ( $\bar{s}s$  vector),  $\Lambda$ (uds),  $\Lambda_c$  (udc),  $F$  ( $\bar{s}c$  pseudoscalar), and  $F^*$  ( $\bar{s}c$  vector). The fits obtained depend on two input quark masses and two irrelevant parameters. The resulting mass ratios are very sensitive to the input quark masses, and insensitive to the irrelevant parameters. We obtain agreement with the physical spectrum to within 12%, and also sensible dependence on input quark masses as they vary. For a particular choice of quark masses, we obtain

$$m_\psi/m_\phi = 3.09 \quad (3.09)$$

$$m_\psi/m_{\Lambda_1} = 2.7 \quad (2.7)$$

$$m_\psi/m_{\Lambda_C} = 1.35 \quad (1.35)$$

$$m_\psi/m_F = 1.34 \quad (1.48)$$

$$m_\psi/m_{F^*} = 1.34 \quad (1.53)$$

We begin by introducing the lattice theory and defining its degrees of freedom. The vacuum is then constructed and the actions of various terms of the interaction hamiltonian are displayed. The treatment of the mass term is discussed. Strong coupling wavefunctions for various particles are then formed, and the perturbation series is constructed and interpreted via Padé approximants. Finally, I present the results and discuss them.

## II. INTRODUCTION TO THE LATTICE THEORY

Quantum chromodynamics is described by the Lagrangian

$$\mathcal{L} = \bar{\psi}(i\not{A} - m)\psi - e\bar{\psi}\gamma_{\mu}\psi A_{\mu} - \frac{1}{4}F_{\mu\nu}F^{\mu\nu} .$$

The theory is asymptotically free and is expected to involve strong coupling at large distances. The lattice formulation of this theory, invented by Wilson and Polyakov,<sup>3</sup> is a natural setting for studying the strong coupling limit. In what follows, we will do some calculations in the Hamiltonian formulation<sup>4</sup> of the lattice gauge theory. This formalism was introduced by Kogut and Susskind.

The Hamiltonian version of the theory is built on a spatial lattice with lattice spacing  $a$  and  $N$  links. Time evolution is continuous. To simplify the canonical formalism and get a Hamiltonian, we will work in the  $A_0 = 0$  gauge.

The degrees of freedom of the theory are  $\psi(r)$  and  $U$ .  $\psi(r)$  is a discretized fermion field, defined on lattice sites  $r$ . The  $U$ 's are matrices in the gauge group. For us, they will be  $3 \times 3$   $SU(3)$  matrices, acting on the color indices of the fermion field. They are labeled  $U(r, \hat{n})$  where  $r$  is a lattice site and  $\hat{n}$  is a lattice direction. We assume  $U(r, n) = U(r+\hat{n}, -\hat{n})^{-1}$ .

Gauge transformations in the lattice theory are

$$\psi(r) \rightarrow V(r)\psi(r)$$

$$U(r, n) \rightarrow V(r) U V^{\dagger}(r + \hat{n}) .$$

Thus, products of fermion fields at different sites are not gauge invariant. Such products will arise when we convert the derivatives of the Dirac Hamiltonian to finite differences. This catastrophe can be averted by noting that the quantity

$$\psi^\dagger(r) U(r, \hat{n}) \psi(r + \hat{n})$$

is a gauge invariant. There is an analogous construction in the continuum theory. It is the gauge invariant definition of a current as a limit given by Schwinger. This uses the form

$$\psi^\dagger(x) \exp \left( ig \int_y^x dz^\mu A_\mu^i(z) (\lambda^i/2) \right) \psi(y)$$

which is gauge invariant for any x and y. In fact, in the continuum limit of the lattice theory, the U matrices approach 1, and can be written

$$U \sim \exp \left( iag A_\mu^i(r) n^\mu (\lambda^i/2) \right) \quad (2.1)$$

as  $a \rightarrow 0$ . This is similar in form to the above. In fact, the various terms in the lattice Hamiltonian are determined in detail by requiring that a naive continuum limit obtained by using the above parametrization of U agrees with the classical Hamiltonian.

The Hamiltonian for the pure gauge theory is

$$H = \frac{g^2}{2a} \sum_{r, \hat{n} > 0} E^2(r, \hat{n}) - \frac{1}{g^2 a} \sum_{\text{squares}} (\text{Tr } UUUU + \text{hc}) \quad .$$

The trace term is an abbreviation for

$$\text{Tr } U(r, \hat{n}) U(r + \hat{n}, \hat{m}) U(r + \hat{n} + \hat{m}, -\hat{n}) U(r + \hat{m}, -\hat{m}) \quad .$$

The first term in H is the electric field strength energy. In our lattice theory, it is the quadratic casimir operator for SU(3). This is because the electric field,  $E_i$  is

the canonical conjugate to  $A_i$  in the continuum theory. From Eq. (2.1) we see that we can generalize  $E$  as the conjugate variable to a degree of freedom  $\Omega$  where  $U = e^{i \cdot \frac{1}{2} \vec{\lambda} \cdot \vec{\Omega}}$ . This gives it the property of generating infinitesimal  $SU(3)$  rotations, so  $E^2$  is the quadratic casimir operator. Note that for various representations  $E^2$  takes on well-defined values. For the singlet,  $E^2 = 0$ ; for the  $\underline{3}$ ,  $E^2 = 4/3$ ; for the  $\underline{6}$ ,  $E^2 = 10/3$ , etc.

The trace over 4  $U$ 's reduces to the non-Abelian magnetic field strength energy in the (classical) limit  $a \rightarrow 0$ . The coefficients recorded are the ones needed to recover the classical continuum Hamiltonian in that limit.

The quantum mechanics is defined by

$$\{\psi_m^\dagger, \psi_n\} = \delta_{mn}$$

$$[E_i, U_{ab}] = \left(\frac{\lambda^i}{2}\right)_{ac} U_{cb} \quad (U \text{ is in the } 3 \times 3 \text{ representation}) \quad .$$

Eventually, we will classify terms in the Hamiltonian into free and interacting parts:  $H = H_0 + xV$ . Then, we'll do perturbation theory in  $V$ .

A particularly convenient setting for high order perturbation calculations is the Wigner-Brillouin<sup>9</sup> formalism. The advantage of this formalism is that it allows systematic high order expansions. If the energy of the state to be computed is  $E$ , and the state in the absence of  $V$  (e.g.  $x = 0$ ) has energy  $E_0$ , we have

$$E = E_0 + \langle V \rangle + \langle V \frac{\pi}{E-H_0} V \rangle + \dots + \langle V \frac{\pi}{E-H_0} V \dots V \frac{\pi}{E-H_0} V \rangle + \dots \quad .$$

$\pi$  is a projection operator excluding the initial state. Note that the energy denominators involve  $E$ , not  $E_0$ . If we assume an expansion,

$$E = E_0 + \alpha_1 x + \alpha_2 x^2 + \dots$$

substitute it in the energy denominators, and expand the result, we can obtain expressions for the  $\alpha_i$ 's. These turn out to be  $n^{\text{th}}$  order matrix elements with energy denominators involving  $E_0$ , and subtractions. These subtractions are important. We shall see that they insure that  $N^2$  contributions to the vacuum energy are cancelled and that particle energies are  $N$ -independent.

Much of our work will involve a slightly more complicated case than the above. We will be considering two degenerate states which are mixed by the perturbation. In this case, we form a matrix  $\omega_{ab}$  with diagonal elements involving the above matrix elements in one of the states and the off-diagonal element involving matrix elements between the two different states. Then we diagonalize the resulting matrix computing its eigenvalues as power series whose coefficients have  $E$ -dependent energy denominators.  $E$  is converted to  $E_0$  as before, with resulting non-trivial subtractions cancelling unwanted  $N$  dependences.

At this point, we are left with power series in  $1/g^2$  for the masses of particles. In the continuum limit, by asymptotic freedom arguments, the bare coupling constant  $g$  goes to zero, so  $x = 1/g^2$  goes to infinity. These series do not converge for large  $x$ , and we want to extrapolate them. To do this, we will use Padé<sup>10</sup> approximants. Padé approximants have been used with much success in the theory of critical phenomena.<sup>11</sup> In that field, expansions in  $(1/T)$  are computed at high temperatures. Padé approximants are then used to search for critical points, calculate critical temperatures, and even critical exponents. We will use them only to extrapolate mass ratios. These have a known asymptote in the continuum limit; they approach constants. Thus, we will be interested in diagonal Padé's.

The Padé approximants to the series we calculate will turn out to extrapolate through the entire range of  $g$  with no singularity, and in fact, with only a small change in the mass ratios.

### III. THE FERMION METHOD

Putting the Dirac equation on a lattice<sup>8</sup> is an ambiguous procedure. Many techniques exist. The major problem is that the simplest lattice Hamiltonian representing the Dirac equation has excitations with low energy in all corners of the Brillouin zone. In one space dimension, this means that excitations with "momentum" 0 and  $\pi/a$  both have zero energy. The way around this problem we choose is to use a formalism in which the Hamiltonian is interpreted as referring to more than 1 field. In one space dimension, there are two fields corresponding to the two components of a fermion field. In three-space dimensions, we have  $2^3 = 8$  fields corresponding to two 4-component fermion fields.

In the representation

$$\vec{\alpha} = \begin{pmatrix} 0 & \vec{\sigma} \\ \vec{\sigma} & 0 \end{pmatrix} ; \beta = \begin{pmatrix} 1 & 0 \\ 0 & -1 \end{pmatrix} ; \gamma_5 = \begin{pmatrix} 0 & 1 \\ 1 & 0 \end{pmatrix}$$

the Dirac equation takes on the form

$$\dot{\phi} = -(\alpha \cdot \nabla)\phi = - \begin{vmatrix} 0 & 0 & \nabla_2 & \nabla_x - i\nabla_y \\ 0 & 0 & \nabla_x + i\nabla_y & -\nabla_2 \\ -\nabla_2 & \nabla_x - i\nabla_y & 0 & 0 \\ \nabla_x + i\nabla_y & -\nabla_2 & 0 & 0 \end{vmatrix} \phi$$

Thus

$$\dot{\phi}_1 = -\nabla_z \phi_3 - \nabla_x \phi_4 + i\nabla_y \phi_4, \text{ etc.}$$

We see that  $\dot{\phi}_i$  involves  $\phi_3$  in the  $\pm\hat{z}$  direction, and  $\phi_4$  in the  $\pm x, y$  directions with similar statements holding the rest of the components of  $\phi$ . This suggests the labeling of the lattice shown in Figure 3.1. The lattice approximation to the gradient is  $\nabla_{\hat{n}}\phi(r) = (\phi(r+\hat{n}a) - \phi(r-\hat{n}a))/2a$ . Thus,  $\phi_i$  is only defined on sites "i" and is zero elsewhere. Furthermore, the labeling 1234 occurs completely in each  $\hat{y} = \text{const.}$  plane. This suggests that we define two fields  $f_i = \phi_i$  ( $y = \text{even}$ ) and  $g_i = \phi_i$  ( $y = \text{odd}$ ).

The Dirac equation then becomes

$$\dot{f} = \frac{1}{a}(\alpha_x \sin k_x a + \alpha_z \sin k_z a)f + \alpha_y(\sin k_y a)g$$

$$\dot{g} = \frac{1}{a}(\alpha_x \sin k_x a + \alpha_z \sin k_z a)g + \alpha_y(\sin k_y z)f$$

Defining  $u = f+g$  and  $d = U(f-g)$ ,

$$\begin{pmatrix} \dot{u} \\ \dot{d} \end{pmatrix} = \alpha_i \frac{(\sin k_i a)}{a} \begin{pmatrix} u \\ d \end{pmatrix} \quad (3.1)$$

where  $U = -\beta\alpha_1\alpha_3$  is a unitary transformation. The continuum limit of this equation is the 2 species Dirac equation. The Hamiltonian in terms of  $\phi$  is not symmetric. We can make a new field

$$\phi(r) = S(r)\chi(r)$$

in terms of which, the Hamiltonian is simpler.  $S(r)$  is a phase. In terms of  $\chi$ ,

$$H = \frac{1}{2a} \sum_r \chi^\dagger(r) \left[ (-)^x \Delta_y + (-)^y \Delta_z + (-)^z \Delta_x \right] \chi(r) \quad (3.2)$$

where  $\Delta_x \phi(r) = \phi(r+\hat{x}) + \phi(r-\hat{x})$ . The phase used was

$$S(r) = i^{r_x+r_z} A_y D(x, z) ; A_y = (-)^{\lfloor \frac{1}{2}y \rfloor} ;$$

$$D(x, z) = -1 \quad \text{if } x \text{ and } z \text{ are odd; } +1 \text{ otherwise} \quad .$$

This is the Hamiltonian used in extensive spectrum calculations reported in reference 8.

The commutation relations obeyed by the Dirac field are

$$\{ \chi_r^\dagger, \chi_{r'} \} = \delta_{rr'} \quad .$$

There is one additional ingredient which we need. We are doing calculations in which the quarks are given a mass. Hence, we want the lattice version of

$$H_m = M_c \bar{c}c + M_s \bar{s}s$$

where c and s are the charmed and strange quark fields. Note that if  $M_c \neq M_s$ , the isospin symmetry of the theory is lost. Explicitly, from Eq. (10.1) we find

$$H_m = (M_c + M_s) \sum_r (-)^{r_x} \chi^\dagger(r) \chi(r) + i(M_c - M_s) \sum_r (-)^{r_x} \chi^\dagger(r) \left[ \Delta_{d_1} - \Delta_{d_2} \right] \chi(r) \quad (3.3)$$

where  $d_1 = \hat{x} + \hat{y}$ ;  $d_2 = \hat{x} - \hat{y}$ ; and  $\Delta_d \chi(r) = \chi(r+d) + \chi(r-d)$ .

The symmetry breaking term in H is nonlocal. This is related to the fact that the original two fields f and g (which occupied different  $\hat{y}$  planes) were coupled, and the decoupled versions, u and d, were mixtures. Note that the action of this term

in  $H$  (to be called  $H_\Delta$ ) is restricted to  $z = \text{constant}$  planes. We shall soon see how the usual space time and internal symmetries appear in this theory.

Finally, we must include the light quarks in this calculation. They are expected to have effects on the spectrum of heavy quarks. Also we will compute the masses of some particles involving both light and heavy quarks. The light quark field will be denoted by  $X$ . All in all, we take as our strong coupling Hamiltonian (preliminarily):

$$H = H_0 + H_h + H_H + H_{\text{box}} + H_\Delta \quad (3.4)$$

where

$$H_0 = \frac{g^2}{2a} \sum_{r, \hat{n} > 0} E^2(r, \hat{n}) + (M_C + M_S) \sum_r (-)^r \chi^\dagger(r) \chi(r)$$

$$H_h = \frac{1}{2a} \sum_r (-)^{r_x} \chi^\dagger(r) U(r, \hat{n}_y) \chi(r + \hat{n}_y) + \dots$$

$$H_H = \frac{1}{2a} \sum_r (-)^{r_x} \chi^\dagger(r) U(r, \hat{n}_y) \chi(r + \hat{n}_y) + \dots$$

$$H_\Delta = i(M_C - M_S) \sum_r (-)^{r_x} \left[ \chi^\dagger(r) U(r, \hat{n}_x) U(r + \hat{n}_x, \hat{n}_y) \chi(r + \hat{n}_x + \hat{n}_y) + \dots \right]$$

$$H_{\text{box}} = -\frac{1}{g^2 a} \sum (\text{tr } UUUU + \text{h.c.})$$

It is convenient to define  $H = g^2/2a W$ .

## IV. THE VACUUM

The ground state of the Hamiltonian  $H_0$  will now be considered. For the pure gauge field, we want to minimize  $E^2(r, \hat{n})$  for each  $r, \hat{n}$ . This is realized by  $E^2 = 0$ . Each link is in the singlet representation. In the absence of a mass term,  $H_0$  makes no reference to fermions, so there is a degeneracy. To resolve it, we must do degenerate perturbation theory to second order. For the moment, consider just one fermion field. In that case, we have to minimize the expression

$$\langle W_{\text{eff}} \rangle = x^2 \langle H_h - \frac{1}{H_0} H_h \rangle$$

$$W_{\text{eff}} = \frac{1}{4} x^2 \sum_{r, \hat{n} > 0} \rho(r) \rho(r + \hat{n}) \quad (4.1)$$

where  $\rho(r) = [\chi^\dagger(r), \chi(r)]$ .

Using the commutation relations for  $\chi$ , we can map out the spectrum of  $\rho$ . It is local, so we shall drop the index  $r$  for now. Let  $|\uparrow\rangle$  be the state for which  $\chi_i |\uparrow\rangle = 0$ . Then,

$$\rho |\uparrow\rangle = -\chi_i \chi_i^\dagger |\uparrow\rangle = -(\{\chi_i, \chi_i^\dagger\} - \chi_i^\dagger \chi_i) |\uparrow\rangle = -3 |\uparrow\rangle$$

$$\rho \chi_a^\dagger |\uparrow\rangle = -\chi_a^\dagger |\uparrow\rangle$$

$$\rho \epsilon_{abc} \chi_a^\dagger \chi_b^\dagger |\uparrow\rangle = +\epsilon_{abc} \chi_a^\dagger \chi_b^\dagger |\uparrow\rangle$$

$$\rho \epsilon_{abc} \chi_a^\dagger \chi_b^\dagger \chi_c^\dagger |\uparrow\rangle = +3(\epsilon_{abc} \chi_a^\dagger \chi_b^\dagger \chi_c^\dagger) |\uparrow\rangle = +3 |\uparrow\rangle$$

The vacuum in this case is seen to be

$|\uparrow\rangle$  for  $r$  odd (even) and  $|\downarrow\rangle$  for  $r$  even (odd) .

It is twofold degenerate, and has an energy  $-\frac{9}{4} N x^2$ .

The two species case is potentially troublesome,<sup>12</sup> but no real difficulties occur for the case at hand. The mass term in  $H_0$  lifts the degeneracy in the heavy quark sector. The resulting vacuum is staggered with  $\rho_H = +3$  on odd sites. This is a first order effect. Next, we look in second order to resolve the remaining light quark degeneracy. Arguments similar to the one field case show that the light quark sector's vacuum is also staggered.

Even though the heavy and light quark vacua are staggered, their relative relationship is still undetermined. The question is whether it is energetically favorable to have heavy and light quark excitations appearing at one site, or heavy quark and light antiquark excitations on one site. The difference is first felt in 4th order. The mass term has no effect.

The only difference between the two vacua to 4th order is whether the allowed representations in the intermediate state of Figure 4.1 are the 1 and 8 or the  $\bar{3}$  and 6. The 1 and 8 come from a vacuum in which quarks and antiquarks of the other species are one site. The  $\bar{3}$  and 6 come from a vacuum which has quarks of all species on one site. The contributions to  $E_0$  are (dropping  $N$  and some numerical factors)

$$\frac{3}{\frac{4}{3} + A} + \frac{6}{\frac{10}{3} + A} < \frac{1}{A} + \frac{8}{3 + A} \quad . \quad (4.2)$$

These are multiplied by (-) in their contribution to  $E_0$ , so clearly, the 2nd vacuum (with the 1 and 8) is favored. We shall use it in our subsequent calculations.

Furthermore, we will retain a  $\rho \cdot \rho$  term for both heavy and light quarks, but added as an irrelevant operator. The coefficients for each will be considered

independent. Keeping these terms in  $H$  is helpful because it lifts the above degeneracies explicitly. They are irrelevant terms in the continuum limit and we shall see that the spectrum in the continuum limit is insensitive to the strength of their coefficients.

## V. ACTIONS OF TERMS IN $H$

Now that we have our vacuum, it is appropriate to see how  $H$  acts on it. First of all, we have those terms arising from the continuum kinetic energy,  $H_h$  and  $H_H$ . They involve bilinears in the fermion field like

$$\chi_i^\dagger(t) U_{ij}(r, \hat{n}) \chi_j(r + \hat{n}) + \text{h.c.} \quad (5.1)$$

Acting on the vacuum, this term produces a quark-antiquark pair with a flux link ( $U_{ij}$ ) between them. This is true for  $\chi$  and  $X$ . Its action will be denoted by Figure 5.1. Also Eq. (5.1) can destroy such an excitation. Appearing in  $H_h$ , such terms are accompanied by a phase. This must be taken into account in doing perturbation theory.

The term involving a product of 4  $U$ -matrices around a square can act upon the vacuum to excite 4 links. The mass term in  $H_0$  appears in energy denominators. It counts of the number of heavy particles in an intermediate state and gives a contribution  $2M_x \times$  that number. The flux energy  $E^2$  is  $4/3$  for the 3 representation. More nontrivial is the action of  $H_\Delta$ .  $H_\Delta$  can destroy a quark and recreate it 2 sites away, in directions  $\pm d_{1,2}$ . For the direction  $\pm d_1$ , we have a  $+iM_x$ , and for  $\pm d_2$ , it is  $-iM_x$ . There is also a phase  $(-)^{r_x}$  where  $r_x$  is the  $x$ -component of the new position of the (anti) quark. Note that these actions are only in the  $x$ - $y$  plane. In making the pure fermion part gauge invariant, we must stretch

gauge field matrices  $U$  from  $r$  to  $r \pm 1$ . This is done both ways (within the plane) and averaged. Finally, in  $H_0$  we now will include  $\rho \cdot \rho$  terms for heavy and light quarks with coefficients  $R_L$  and  $R_H$ . These terms assign different energies to different fermion configurations. Thus, a graph like Figure 5.2 is well defined. The vacuum has an energy due to the  $\rho \cdot \rho$  term which comes about because  $\rho = \pm 3$  for each site, and adjacent sites have opposite signs. Thus, the vacuum expectation value of the  $\rho \cdot \rho$  term is  $(3)(-3) \times$  the number of links on the lattice. A fermion on a site changes its  $\rho$ -value from  $-3$  to  $-1$ . The 6 links which each had the value  $(-9)$  now have the value  $(+3)(-1) = -3$ , each increasing in energy by  $6R$ . A single fermion has an energy  $36R$ . One can compute the  $\rho \cdot \rho$  energy for various fermion configurations in this fashion.

## VI. TREATMENT OF THE MASS TERM

In the rescaled Hamiltonian  $W$ , the mass terms appear as  $Ma/g^2$ . We now discuss the continuum limit of this.

The running coupling constant in lattice gauge theories is conjectured to behave linearly for large  $a$  until some point  $g = O(1)$  where it starts to fall off more slowly than linearly. It is unlikely that a 4th order calculation will be extrapolated into this region. The calculations<sup>13</sup> which indicate this dependence show that  $g$  departs from linear behavior in the correct direction, but are not reliable beyond that. We must be content to extrapolate a strongly coupled theory  $g \gg 1$  ( $x \ll 1$ ) to a fairly weakly coupled theory. It is our hope that the hadron masses are insensitive to the  $g \ll 1$  region, and that the dynamics responsible for hadron masses takes place at larger distances. Operationally, this means we take  $g(a) \propto a$  for purposes of taking a continuum limit.

Another issue is mass renormalization in a non-superrenormalizable theory in the strong coupling regime. The Gross-Neveu model has been studied on the

lattice. Recall this is a many species version of the Thirring model. With an appropriate choice of the sign of the coupling, the theory is asymptotically free. The theory is described by the Lagrangian

$$\mathcal{L} = \bar{\psi}(i \not{\partial}) \psi + \frac{1}{2} g^2 (\bar{\psi} \psi)^2$$

Zee,<sup>14</sup> and Shigemitsu and Elitzur<sup>6</sup> have analyzed this model in the Hartree-Fock approximation. They find an integral equation for the "gap"  $-g^2 \langle \bar{\psi} \psi \rangle$ . By holding this "gap" or effective fermion mass constant with varying cutoff (in the Hartree-Fock approximation), they are able to reproduce the correct behavior for the running coupling constant in both strong and weak coupling limits. A bare mass added to the above theory is not a drastic perturbation since the theory without a bare mass spontaneously breaks chiral symmetry by generating a fermion mass. One can show that the effect of adding a bare mass is just to add it to the gap in the integral equation, producing an effective gap. The treatment of the gap as constant, independent of  $a$  then translates to treating the effective gap also as independent of  $a$ .

The mass renormalizations from the strong coupling end are seen to be similar to that of the Schwinger model. We must go one step further. The Schwinger model, or our 4-dimensional theory with  $M = \text{constant}$  has a mass term like  $Ma/g^2$ . In these theories, we have  $g \propto a$ . The net coefficient of the mass term is then  $M\sqrt{\kappa}$ . In the four dimensional theory, this would mean we need 8 orders of perturbation theory in the mass term. Such a calculation is not feasible. We must be content to use a coefficient  $Mx$ . To see how dramatic this concession is, we carried it out for the Schwinger model.

The spectrum of the massless Schwinger model consists of free bosons of mass  $(e^2/\pi)$ . When a fermion mass is included, there is an attractive interaction in the scalar sector of the two boson state. This attraction binds the two bosons, forming the scalar state of the massive Schwinger model. Both strong and weak coupling limits of the binding energy of this state are amenable to exact continuum analysis.<sup>5</sup> Furthermore, there exists an approximate continuum calculation for the binding energy of the scalar state for all fermion mass.<sup>15</sup> It is a variational calculation done in the infinite momentum frame when the theory is particularly simple. Of course, it agrees with both (exactly known) limits. The binding energy is essentially a mass ratio, and precisely the kind of quantity we wish to calculate using strong coupling methods. Fig. 6.1 displays the results of both the variational continuum calculation (the lower curve) and the strong coupling calculation using a mass term  $Mx$ . These results are very encouraging, and we will treat the mass term in four dimensions accordingly.

Our Hamiltonian now is (with  $g^2/2a$  scaled out)

$$\begin{aligned}
 H_0 &= \sum_{r, \hat{n}} E^2(r, \hat{n}) + M_+ x \sum_r (-)^r \chi^\dagger(r) \chi(r) + RL \sum_{r, \hat{n} > 0} \rho_L(r) \cdot \rho_L(r + \hat{n}) \\
 &\quad + RH \sum_{r, \hat{n} > 0} \rho_H(r) \cdot \rho_H(r + \hat{n}) \\
 H_h + H_H &= x \sum_{r, \hat{n}} P(\hat{n}) \left[ \chi^\dagger(r) U(r, \hat{n}) \chi(r + \hat{n}) + \dots \right] \\
 H_\Delta &= iM_- x \sum_r (-)^r x \left[ \chi^\dagger(r) U(r, \hat{n}_x) U(r + \hat{n}_x, \hat{n}_y) \chi(r + \hat{n}_x + \hat{n}_y) + \dots \right] \\
 H &= -2x^2 \sum_{\text{boxes}} (\text{Tr } UUUU + \text{h.c.}) \quad . \quad (6.2)
 \end{aligned}$$

## VII. THE 4TH ORDER VACUUM

With our Hamiltonian, we can now illustrate the computation of the vacuum energy to 4th order in  $x$ . To order  $x$ , there is no contribution. To order  $x^2$ , we have the graphs of Figure 7.1. They contribute

$$x^2 \cdot 3 \cdot N \cdot \left( \frac{-1}{\frac{4}{3} + 68RL} \right) + x^2 \cdot 3 \cdot N \cdot \left( \frac{-1}{\frac{4}{3} + 68RH + 4M_x} \right) .$$

The three comes from the fact that the color group is SU(3), e.g.

$$\langle U_{ij}^\dagger U_{kl} \rangle = \frac{1}{3} \delta_{il} \delta_{jk}$$

and multiplying this by  $\delta_{il} \delta_{jk}$  yields 3. The N comes from the fact that there are N-links on the lattice. The energy denominator's  $4/3$  is the expectation value of  $E^2$  in the triplet state created by U. The 68RL,RH come from the 2 quarks. To see this, note that there are 10 links from a quark outward to undisturbed vacuum yielding  $6 \cdot 10 = 60$ . The remaining link, from one quark to the antiquark, has a  $\rho \cdot \rho$  term of (-1) as opposed to (-9), so this link is +8 above the vacuum. Thus, the  $\rho \cdot \rho$  energy of the configuration is +68.

To third order, we might have a graph like Figure 7.2. It is not hard to see that the sum of such graphs vanishes. Next, we come to 4th order. Graphs like Figure 7.3 come in many varieties. There are N places to put the first. It turns out that there are N-57 places to put the second bubble with a  $\rho \cdot \rho$  energy of the configuration being  $2 \cdot 68 = 136R$ , 42 places with  $\rho \cdot \rho = 132R$ , four with  $\rho \cdot \rho = 128R$ , 10 places which touch the original link, having a  $\rho \cdot \rho$  term of 128R, and the one way to put the second bubble on the original link, with a  $\rho \cdot \rho$  energy of 128R. For the graphs with disjoint vacuum bubbles, the 3 from SU(3)-color is now a

9. For those graphs which have the bubbles touching, the factor is a 6. The graph with the second bubble on the same link as the first will have its intermediate state with flux in the  $\bar{3}$  representation, so  $E^2$  for it is  $4/3$  in contrast to the others which have  $4/3$  from each of 2 links. Note that  $\underline{3} \times \underline{3} = \bar{\underline{3}} + \underline{6}$ , and conceivably the intermediate flux state could be a  $\underline{6}$ . This is forbidden, however, because of the antisymmetry involved in having 2 fermions on one site.

Time orders also have to be included. They give a factor of 4 for all graphs except the one with both bubbles on one site. All in all, these diagrams give

$$\begin{aligned}
 & - \frac{12N}{\left(\frac{4}{3} + 68RL\right)^2 \left(\frac{4}{3} + 128RL\right)} - \frac{192N}{\left(\frac{4}{3} + 68RL\right)^2 \left(\frac{8}{3} + 128RL\right)} \\
 & - \frac{756N}{\left(\frac{4}{3} + 68RL\right)^2 \left(\frac{8}{3} + 132RL\right)} - \frac{18N(N-57)}{\left(\frac{4}{3} + 68RL\right)^2 \left(\frac{8}{3} + 136RL\right)} .
 \end{aligned}$$

Then, we have diagrams with one bubble of light quarks and the other consisting of heavy quarks. One such diagram's essential features appeared in Eq. (4.2). We shall see how that came about. The intermediate state can be in a  $\underline{1}$  or an  $\underline{8}$  now. This is because the 2 species are on different lattice sites, so we have  $\underline{3} \times \bar{\underline{3}} = \underline{1} + \underline{8}$  (as opposed to  $\underline{3} \times \underline{3} = \bar{\underline{3}} + \underline{6}$ ). The energy denominator for a  $\underline{1}$  has  $E^2 = 0$ , and a regular  $\rho \cdot \rho$  energy. The  $\underline{8}$  has  $E^2 = 3$ . The only new feature is the coefficients which appeared in Eq. (4.2). The matrix element needed is

$$\langle U_{ba}^\dagger U_{dc} U_{cd}^\dagger U_{ab} \rangle$$

(see Figure 4.1). One may insert a projection operator in the middle of this to extract the  $\underline{1}$  or  $\underline{8}$  representations. These have different energy denominators. Recall the Clebsh-Gordon series for a product of U's:

$$U_{ab}U_{cd} = \sum \langle Na, Mc | R\alpha \rangle \langle Nb, Md | R\beta \rangle U_{\alpha\beta}^R .$$

We also have the Clebsh-Gordon coefficients

$$\langle 1 | 3i, \bar{3}j \rangle = \frac{1}{\sqrt{3}} \delta_{ij}$$

$$\langle 8, \alpha | 3i, \bar{3}j \rangle = \frac{1}{\sqrt{2}} \lambda_{ij}^{\alpha} .$$

Thus, in the above, a singlet contributes

$$\left( \frac{1}{3} \delta_{cb} \delta_{ad} \right) \left( \frac{1}{3} \delta_{cb} \delta_{ad} \right) = 1 .$$

The octet contributes:

$$\langle \bar{3}a, 3d | 8\alpha \rangle \langle \bar{3}b, 3c | 8\beta \rangle \langle \bar{3}d, 3a | 8\gamma \rangle \langle \bar{3}c, 3b | 8\delta \rangle \langle U_{\alpha\beta}^8 U_{\gamma\delta}^8 \rangle$$

$$= \frac{1}{8} \frac{1}{4} \lambda_{ad}^{\alpha} \lambda_{bc}^{\beta} \lambda_{da}^{\gamma} \lambda_{cb}^{\delta} \delta_{\alpha\gamma} \delta_{\beta\delta}$$

$$= \frac{1}{32} \left( \lambda_{ad}^{\alpha} \lambda_{da}^{\alpha} \right) \left( \lambda_{bc}^{\beta} \lambda_{cb}^{\beta} \right) = \frac{1}{32} 16 \cdot 16 = 8 .$$

More complicated matrix elements of U's are handled similarly.

Finally, we have those terms possible due to the new mass-difference operator in the Hamiltonian. These differentiate between "sticks" created by  $\chi^{\dagger}(r)U_{\chi}(r + \hat{d})$  in the x, y, and z directions. For those in the x or y direction, we have a group of diagrams shown in Figure 7.4. They contribute

$$-\frac{2}{3} NM_-^2 \cdot 36 \cdot \left( \frac{1}{\frac{4}{3} + 68RH + 4M_+x} \right)^2 \left( \frac{1}{4 + 72RH + 4M_+x} \right) .$$

The  $2/3$  is because  $2/3$  of the links are in the x-y plane. The remaining links are in the  $\hat{z}$  direction. Their contribution is also evaluated as

$$-\frac{1}{3} NM_-^2 \cdot 48 \cdot \left( \frac{1}{\frac{4}{3} + 68RH + 4M_+x} \right)^2 \left( \frac{1}{4 + 72RH + 4M_+x} \right) .$$

There is also a contribution from  $H_{\text{box}}$  which is  $\frac{3}{2} N$ . Then, we have the subtractions in the Wigner-Brillouin formalism. These in this case correspond to adding

$$-\langle V \frac{1}{E_0 - H_0} V \rangle \langle V \frac{1}{(E_0 - H_0)^2} V \rangle .$$

For the vacuum, these reduce to adding

$$9N^2 \left[ \frac{1}{\frac{4}{3} + 68RL} + \frac{1}{\frac{4}{3} + 68RH + 4M_+x} \right] \left[ \left( \frac{1}{\frac{4}{3} + 68RL} \right)^2 + \left( \frac{1}{\frac{4}{3} + 68RH + 4M_+x} \right)^2 \right] .$$

When this is done, all  $N^2$  dependence disappears from the computed shift in the vacuum energy and it has its proper extensive nature. The next task is to compute the particle spectrum above the vacuum. Before turning to this, we will take a second look at the lattice fermion method.

VIII. SYMMETRIES OF THE FERMION HAMILTONIAN<sup>8</sup>

Consider one species, and its Hamiltonian

$$H = \frac{1}{2a} \sum_r \chi^\dagger(r) \left[ (-)^{r_x} \Delta_x + (-)^{r_y} \Delta_y + (-)^{r_z} \Delta_z \right] \chi(r) .$$

This Hamiltonian incorporates many fermion symmetries, but in a complicated manner. In the first place, we have translation and parity. Translation symmetry, because of the labeling of the lattice, is  $r \rightarrow r + 2\hat{n}$ .

Another symmetry of  $H$  is translation by one unit in a given direction. In order to recover the original Hamiltonian, we must incorporate a phase:

$$\begin{aligned} & (-)^{r_z} \chi(r + \hat{n}_y) \\ \chi(r) \rightarrow & (-)^{r_x} \chi(r + \hat{n}_z) . \\ & (-)^{r_y} \chi(r + \hat{n}_x) \end{aligned}$$

This takes the  $u$  and  $d$  fields to (for the last case)

$$u \rightarrow i \begin{pmatrix} d_3 \\ d_4 \\ d_1 \\ d_2 \end{pmatrix} , \quad d \rightarrow i \begin{pmatrix} u_3 \\ u_4 \\ u_1 \\ u_2 \end{pmatrix}$$

and corresponds to  $i\gamma_5\tau_1$ . Translations in the  $\hat{y}$  or  $\hat{z}$  directions in Eq. (8.1) correspond to  $i\gamma_5\tau_2$  or  $i\gamma_5\tau_3$ . We can also combine these:  $(i\gamma_5\tau_1)(i\gamma_5\tau_2) = -\tau_1\tau_2 = -\tau_3$ .

$$\tau_3: \chi(r) \rightarrow -i (-)^{r_z+r_y} \chi(r + \hat{n}_x + \hat{n}_y)$$

Note that these satisfy ordinary product rules as they must.

Consider a lattice rotation. Only lattice rotations of  $90^\circ$  about an axis, which can be a symmetry of the lattice, are to be considered. If we make an ansatz

$$\chi(r) \rightarrow P(r)\chi(r')$$

we can determine what conditions P must satisfy to keep H invariant. For lattice rotations of just  $90^\circ$ , we can show that such a P exists, and  $90^\circ$  lattice rotations correspond to  $\exp\left(\frac{i\pi}{4}(\sigma + \tau) \cdot \hat{n}\right)$  on the quark fields u and d. It is more convenient to consider rotations about an axis of  $\pi$ , which on the quark fields is  $\exp\left(\frac{i\pi}{2}(\sigma + \tau) \cdot \hat{n}\right) = i(\vec{\sigma} + \vec{\tau}) \cdot \hat{n}$ . We can then undo the isospin transformation, and come up with pure spin operators on u and d:

$$i\sigma_x: \chi(xyz) \rightarrow (-)^{r_x+r_z} \chi(x, 1-y, 1-z)$$

$$i\sigma_y: \chi(xyz) \rightarrow -(-)^{r_x+r_y} \chi(1-x, y, 1-z)$$

$$i\sigma_z: \chi(xyz) \rightarrow (-)^{r_y+r_z} \chi(1-x, 1-y, z) \quad (8.2)$$

These are symmetries of H. These can now be used to classify states.

## IX. SOME WAVEFUNCTIONS

We can construct the wavefunctions of the  $\phi$  and  $\psi$  particles. They are vector mesons which are formed from  $s$  or  $c$  quarks alone. A straightforward way to find their wavefunctions is to write out the bilinear  $\bar{c}\gamma_\mu c$  or  $\bar{s}\gamma_\mu s$  in terms of  $f_i$ ,  $g_i$ , and then in terms of  $\chi$ . The component we choose is  $\mu = x$ . Let

$$|A\rangle = \frac{1}{\sqrt{3}} i \sum_r (-)^{r_z} \left[ \chi^\dagger(r)\chi(r+n_x) - \chi^\dagger(r+n_x)\chi(r) \right]$$

$$|B\rangle = \frac{1}{\sqrt{3}} \sum_r (-)^{r_y} \left[ \chi^\dagger(r)\chi(r+n_y) + \chi^\dagger(r+n_y)\chi(r) \right] .$$

Then,

$$|\phi\rangle = \frac{1}{\sqrt{2}} (|A\rangle - |B\rangle)$$

$$|\psi\rangle = \frac{1}{\sqrt{2}} (|A\rangle + |B\rangle) .$$

Now, the two components of each wavefunction are degenerate to zeroth order.

They are mixed by  $H_\Delta$  in first order because

$$\langle A | H_\Delta | B \rangle = 4M_- .$$

One can see this as follows.  $|B\rangle$  consists of sticks in the  $\hat{y}$  direction, with a phase  $(-)^{r_y}$  where  $r_y$  is taken from the point closest to  $y = -\infty$ .  $|A\rangle$  consists of sticks in the  $\hat{x}$  direction with a phase  $i(-)^{r_z}(-)^r$  or  $i(-)^{r_x+r_y}$  where  $r$  is the point closest to  $x = -\infty$ . Take an end of the  $y$ -stick and let  $H_\Delta$  move it in a way such that the resulting state can project onto  $\langle A |$ , e.g. take the lower quark which was at  $r$  and

put it at  $r' = r + n_x + n_y$ . Doing this,  $H_\Delta$  gives us a factor  $iM_-(-)^{r_x+1}$ . Then, projecting this onto  $\langle A |$  gives us a factor  $-i(-)^{r_x+r_y+1}$  ( $r$  is the point of origin of the quark we moved), and the net factor is  $+M_-$ . There are two ways of doing this to each of 2 quarks, and the sign for all such processes is positive, and the matrix element is as stated.

When we compute a mass-matrix, we will have a degeneracy in  $|A\rangle$  and  $|B\rangle$ . There is a mixing amplitude  $4M_x$ , and a diagonal amplitude  $\frac{4}{3} + 68RH + 4M_x$  to lowest order. The linear combinations of  $|A\rangle$  and  $|B\rangle$  diagonalizing the mass matrix are  $|A\rangle \pm |B\rangle$  in  $|\phi\rangle$  and  $|\psi\rangle$ . Furthermore, the "0<sup>th</sup>" order energies involved for the  $\phi$  and  $\psi$  respectively involve  $(M_+ M_-)$  which is  $M_s$  or  $M_c$  alone.

Similarly, we can compute the wavefunctions for vector and pseudoscalar mesons consisting of c and s quarks. We have

$$|A, F\rangle = \frac{1}{\sqrt{3}} \sum (-)^{r_x+r_y} \left[ \chi^\dagger(r) \chi(r + \hat{n}_y) + \chi^\dagger(r + \hat{n}_y) \chi(r) \right] |0\rangle$$

$$|B, F\rangle = i \frac{1}{\sqrt{3}} \sum (-)^{r_x+r_z} \left[ \chi^\dagger(r) \chi(r + \hat{n}_x) + \chi^\dagger(r + \hat{n}_x) \chi(r) \right] |0\rangle$$

$$|F\rangle = \frac{1}{\sqrt{2}} (|A, F\rangle - |B, F\rangle)$$

$$|A, F^*\rangle = -i \frac{1}{\sqrt{3}} \sum (-)^{r_x+r_y} \left[ \chi^\dagger(r) \chi(r + n_x) + \chi^\dagger(r + n_x) \chi(r) \right]$$

$$|B, F^*\rangle = \frac{1}{\sqrt{3}} \sum (-)^r \left[ \chi^\dagger(r) \chi(r + \hat{n}_y) + \chi^\dagger(r + \hat{n}_y) \chi(r) \right]$$

$$F^* = \frac{1}{\sqrt{2}} (|A, F^*\rangle - |B, F^*\rangle)$$

For the  $F$  and  $F^*$ , the components  $A$ ,  $B$  do not mix to lowest order. The wavefunctions involving  $A$ - $B$  arises from the externally imposed constraint of looking at  $\bar{c}s$  states, but it really makes no difference. The mass involved in lowest order is just  $M_+ \approx M_C + M_S$  as it should be.

## X. THE NUCLEON WAVEFUNCTION

We shall also construct a wavefunction for a nucleon state. The ones most accessible to us are  $udc$  and  $uds$ . Since light and heavy quarks are on staggered sites, it has the structure of a meson. The two light quarks are on one site and the heavy quark is one site away. We can construct wavefunctions which have nonzero  $\langle B | H_\Delta | A \rangle$ , having the correct mass to lowest order. These states are not actually states of definite  $\tau_3$  (heavy) because when one performs the required translations on just the heavy particles, the light ones remain at their sites and a new many link state is mixed into the original. They are, however, truncations to one link of such exact states. Moreover, the critical requirement is that the matrix element  $\langle B | H_\Delta | A \rangle$  give the correct lowest order mass. The structure of the gauge field-fermion complex is  $\chi_i^\dagger(r) X_j^\dagger X_k^\dagger(r + \hat{n}) \epsilon_{\alpha j k} U_{i\alpha}(r, \hat{n})$ . As a convenient ansatz, we take

$$|A\rangle = \sum_r P_A(r) \left[ \chi_i^\dagger(r) X_j^\dagger(r) \chi_k^\dagger(r + \hat{n}_x) + \sigma_x \chi_i^\dagger(r + n_x) X_j^\dagger(r + n_x) \chi_k^\dagger(r) \right] |0\rangle$$

$$|B\rangle = \sum_r P_B(r) \left[ \chi_i^\dagger(r) X_j^\dagger(r) \chi_k^\dagger(r + \hat{n}_y) + \sigma_y \chi_i^\dagger(r + n_y) X_j^\dagger(r + n_y) \chi_k^\dagger(r) \right] |0\rangle .$$

We shall require  $\langle A | H_\Delta | B \rangle = 2M_-$  and also that the states are spin  $\frac{1}{2}$ . They are to be identified with the  $\Lambda$  and  $\Lambda_C$ .

Requiring the nucleon states to have spin  $\frac{1}{2}$  reduces to the conditions

$$P_A(-x, 1-y, z) = -i\sigma_x P_A(r)(-)^{r_y+r_z}$$

and

$$P_B(1-x, -y, z) = -i\sigma_y(-)^{r_x} P_B(r)$$

Then, requiring  $\langle A | H_\Delta | B \rangle = 2M_-$  leads to other conditions allowing a determination of  $P_A(r)$  and  $P_B(r)$ . The resulting wavefunctions describe nucleon states with spin  $\frac{1}{2}$ .

In actual fact, the precise forms of  $P_A$  and  $P_B$  make no difference to 4th order in the strong coupling expansion. The only times such phases are really important are when, to a given order, it is possible to annihilate the particle and recreate it elsewhere. This can be done for the previous particles, but not for the nucleon.

## XI. THE PERTURBATION SERIES

Now we will present some details of the perturbation calculation. To lowest order,  $H_\Delta$  can contribute.  $\langle B | H_\Delta | A \rangle \neq 0$  for some of our particles. This induces mixings, and is the only first order contribution.

In second order, we have standard contributions in which  $H_h$  and  $H_H$  make vacuum bubbles in the presence of a particle. These have been explained in the literature.<sup>8</sup> They are evaluated in much the same way as the 4th order vacuum. Also,  $H_\Delta$  contributes as it did to the 4th order vacuum. One new feature available to the  $\phi$ ,  $\psi$ ,  $F$  and  $F^*$  is annihilation and recreation at some other link. There are phases which come into play from the wavefunctions and from the Hamiltonian itself.

There are some third order graphs. These are shown in Figure 11.1. There is also a contribution from expanding the  $M_+$  terms in second order. Note that the vacuum bubble may be from either species of quark. We will present the third order calculation for  $\psi$  and  $\phi$  in some detail in order to illustrate the methods involved. To begin with, we present a shorthand notation for energy denominators. The flux content is denoted by the first letter. Then, the value of the  $\rho \cdot \rho$  term follows as a number. Finally, the character of the quarks involved is denoted by H or L. Thus,  $A68H = 1/(4/3 + 68RH)$ ,  $B128L = 1/(8/3 + 128RL)$ , etc. These abbreviations are acceptable to a computer.

The last graph in Figure 11.1 can be evaluated yielding

$$-8M_{-}^3(B4H)^2 = 8M_{-}^3(B4H)(B0H) + 4M_{-}(B0H) \quad .$$

The second to last and third to last graphs sum to zero. The first graph, when the vacuum bubble is on the original link of the particle, and is composed of heavy quarks, gives

$$(4M_{-})^4 \cdot 2 (C60H) A60H \quad .$$

The  $4M$  comes from the 4 ways H can act on the particle to make such a graph. The next 4 is a result of the trace on-color indices. The two comes to include the identical contribution we have from the same process occurring on the link occupied by the final particle. The energy denominator  $C60H$  has a flux contribution of zero because the intermediate state it measures is in a  $\bar{3}$  flux state. This is because  $\underline{3} \times \bar{\underline{3}} = \bar{\underline{3}} + \underline{6}$  and the  $\underline{6}$  representation is excluded due to the fact that it is coupled to two fermions on one site which, of course, are automatically

antisymmetrized. The next energy denominator  $A_{60H}$  comes from the configuration resulting after  $H_{\Delta}$  has moved a quark; now there are 2 links in the  $\underline{3}$  representation; the initial state had one, and the difference is a flux energy of  $4/3$ . Next, consider a diagram in which the heavy quark vacuum bubble touches the quark of the original particle unaffected by  $H_{\Delta}$ . There are 4 possible links for this: a factor of  $(4M_-)$  as above, 2 energy denominators  $(-A_{60H})$ , and a color-trace of 2. The result is

$$32 M_- (A_{60H})^2 .$$

There are lots of other places near the particle to put the vacuum fluctuation, and in fact  $(N-74)$  places to put it which have no interaction with the particle. For these, we have the contribution

$$(4M_-)(N-74) 3 (A_{68H})^2 .$$

Furthermore, we have to consider the case of a light quark vacuum fluctuation. When this occurs on one of the two links the particle occupied, the contribution is

$$(4M_-)(A_{68L}) 2 \cdot \frac{1}{3} [ D_{68L} + 8 E_{68L} ] .$$

The energy denominator  $D$  has a flux contribution  $-4/3$  and corresponds to the singlet representation in  $\underline{3} \times \underline{\bar{3}} = \underline{1} + \underline{8}$ . The  $E$  means a flux energy of  $5/3 = 3 - 4/3$  where  $3$  is the quadratic casimir operator for the octet. The weights for each are  $1/3$  and  $8/3$  respectively. In addition to these, we have the results of expanding the second order energy denominators  $1/(4/3 + 68RH + 4M_+ x)$  in  $M_+ x$  to be added to the

above. Finally, there is the subtraction from Wigner-Brillouin perturbation theory. In this case it is

$$-4(M_+ \pm M_-) < A | V \left( \frac{1}{E_0 - H_0} \right)^2 V | B > .$$

The vacuum energy also has a third order contribution due to expanding the second order energy denominator in  $M_+$ . When all of these are combined, the  $N$ -dependence disappears and we have our contribution. This is nothing compared to fourth order.

In fourth order, we have graphs coming from  $H_H^4$ . These include types shown in Figure 11.2. Also, we have graphs in which  $H_\Delta$  acts twice. They include types shown in Figure 11.3. In many of these, vacuum bubbles consisting of light quarks are permitted. The nucleon graphs have a different counting due to their different structure. After computing (and checking!) the myriads of such contributions, we must also collect expansions in  $M_+$  from lower order and the Wigner Brillouin subtraction term. Everything is then put on a computer for numerical evaluation.

## XII. RESULTS

The results of the fourth order calculations for the  $\phi$ ,  $\psi$ ,  $\Lambda$ ,  $\Lambda_c$ ,  $F$  and  $F^*$  were programmed on a computer for repeated evaluation and variation of parameters. The program evaluated terms in the strong coupling expansions, took appropriate ratios, and constructed diagonal Padé approximants. The input was quark masses and the values of the  $\rho \cdot \rho$  terms for light and heavy quarks.

First, the series were analyzed with  $m_c = m_s = 0$ . The series were seen to be "healthy," i.e. extrapolatable. The mass ratios resulting were  $m_\phi/m_\Lambda \approx .9$  and  $m_\phi/m_F \approx 1.0$  at a given value of RH and RL.

Then we varied  $M_+$  and  $M_-$  and computed ratios  $m_\psi/m$ . For  $M_+ = 2.0$ ,  $M_- = 1.65$ ,  $RH = .001$ , and  $RL = .002$ , we have displayed the Padés in Figure 12.1. Note that the continuum limit is reached at  $x \approx 5$ . All ratios at  $x = 0$  start out near 1 and move to continuum values which are quite close (up to a factor of 2) to the  $x = 0$  point. The Padés are smooth and well behaved. Note that the particle masses are all within 12% of their experimental mass ratios.

There is still more to do to understand the character of these mass ratios. First, let's address the irrelevancy of the  $\rho \cdot \rho$  term. For RL, we have the graph displayed in Figure 12.2. When RL varies by a factor of 20, the most dramatic change is shown by the ratio  $m_\psi/m_\Lambda$ . This changes by .6 over the range. The other particles are quite independent of RL. The mass ratios exhibit more dependence on RH, however. This can be understood, since the  $\rho \cdot \rho$  term is similar to the mass term. Both are sources of chiral symmetry breaking. Of course, in the continuum limit, the mass term is huge compared to the  $\rho \cdot \rho$  term, but the fourth order expansion presumably does not see beyond some finite  $x$ .

The mass ratios behave in a very systematic way as functions of the parameters. Consider RL, RH fixed. The ratio  $m_\psi/m_\phi$  increases as  $M_- \rightarrow M_+$  (as

the strange quark gets lighter). For a very wide range of  $M_+$ , we can always find an  $M_-$  to fit the ratio to 3.1. The ratio  $m_\psi/m_\Lambda$  exhibits more dependence on the absolute values of  $M_\pm$ . As these masses increase, so does  $m_\psi/m_\Lambda$ . This is in accord with quark counting. These two facts are the basis of our fits. Given a set of parameters RL and RH, we can find a unique set  $m_+, M_-$  fitting the two above-mentioned ratios. Then we look at the remaining three ratios:  $m_\psi/m_{\Lambda_c}$ ,  $m_\psi/m_F$ ,  $m_\psi/m_{F^*}$ . They are always given by the values in the naive fit Figure 12.1. The masses  $M_\pm$  depend on RL and RH. Once set by the two ratios we use to determine them, the remaining three mass ratios are always given by the fit. This results in an interpretation of the "irrelevancy" of RL and RH. They determine the quark mass parameters. Given them, we fit  $M_\pm$  to data, and the remaining ratios computed are independent of these choices. The fit of  $M_\pm$  by  $m_\psi/m_\phi$  and  $m_\psi/m_\Lambda$  is unique (as seen from experience). In Figure 12.3 we present a graph of  $M_\pm$  (RH). It strongly depends on RH, but this might be thought of as a renormalization point.

The reason we have retained RH was to avoid problems with diagrams like Figure 5.2. Such a diagram has no flux contribution to the energy denominator. When there is no  $\rho \cdot \rho$  term, the only term in the energy denominator is  $M_+ x$ . If we were dealing with massless quarks, such a situation would be indicative of a degeneracy in the meson-exotic sector. The mass term splits these, as does the  $\rho \cdot \rho$  term, so there is no degeneracy. Nevertheless, the mass term alone makes this diagram contribute to a lower order (the energy denominator is proportional to  $x$ ). The calculation of the spectrum with  $RH = 0$  seems feasible, but has not yet been done.

Another aspect of the spectrum presented is the lack of any splitting between  $F$  and  $F^*$ . These are analogs of the  $\pi$  and  $\rho$  for the light quark spectrum. Calculated to fourth order, the spectrum of light quarks shows a very small  $\pi - \rho$

splitting, and this is its chief problem. Of course, in the heavy quark regime, one does not expect the dramatic splitting one sees in the  $\pi$ - $\rho$  system.

Another calculation of interest is to see how mass ratios behave in the limit of large  $M_{\pm}$ . When the quark masses are much more important than the other terms in  $H$ , we expect exceedingly simple mass ratios to result. This does, in fact, occur. From a graphical point of view, contributions like Figure 11.3 are roughly the same for all particles. When series grow very rapidly, Pade's are dominated by low orders. This is what happens here. For the ratio  $m_{\psi}/m_{\phi}$ , with  $M_{+} = 100$  and  $M_{-}$  varying from 0 to 50, the departure of the mass ratio given by the lattice theory from the naive quark mass ratio is 0%. For other ratios, the agreement is not quite so spectacular, but for  $M_{-} \lesssim 20$ , it is good to a few percent.

Finally, we can speculate on techniques which might be useful in computing the K-D type particle masses. Recall these have the property that their zeroth order strong coupling wavefunctions are mixtures with different amounts of flux. Although many things remain to be worked out, perhaps matrix Pade approximants could be of use here.

### XIII. DISCUSSION

We have seen that the mass ratios computed in the lattice gauge theory of heavy quarks are realistic. Their extrapolations from strong coupling to the continuum limit are singularity free. They have sensible behaviors in limits (say, large quark masses) and are quantitatively accurate in a regime of quark masses. There are further calculations which can be done, notably, treating more particles. It does not seem feasible to extend these calculations to higher order by hand, but perhaps the computer work presently underway<sup>16</sup> will be used to shed some light on their behavior.

## ACKNOWLEDGMENTS

I wish to thank J. Kogut for many important conversations and much guidance throughout the course of this work. This work comprised part of my thesis presented to Cornell University.

## REFERENCES

- <sup>1</sup> H. Fritzsch, M. Gell-Mann and H. Lentwylter, Phys. Lett. 47B, 365 (1973).
- <sup>2</sup> G. 't Hooft, Marseilles Conference on Gauge Theories (unpublished); H.D. Politzer, Phys. Rev. Lett. 30, 1346 (1973); D.J. Gross and F. Wilczek, ibid. 30, 1343 (1973).
- <sup>3</sup> K.G. Wilson, Phys. Rev. D10, 2445 (1974); A.M. Polyakov (unpublished) and Phys. Lett. 59B, 82 (1975).
- <sup>4</sup> J. Kogut and L. Susskind, Phys. Rev. D11, 395 (1975).
- <sup>5</sup> T. Banks, L. Susskind, and J. Kogut, Phys. Rev. D13, 1043 (1976); A. Carroll, J. Kogut, D.K. Sinclair and L. Susskind, Phys. Rev. D13, 2270 (1976).
- <sup>6</sup> J. Shigemitsu and S. Elitzur, Phys. Rev. D14, 1988 (1976).
- <sup>7</sup> J. Kogut, D.K. Sinclair and L. Susskind, Nucl. Phys. B114, 199 (1976).
- <sup>8</sup> T. Banks, et al., Phys. Rev. D15, 1111 (1977).
- <sup>9</sup> G. Baym, Quantum Mechanics (W.A. Benjamin, Inc. Massachusetts, 1969).
- <sup>10</sup> G.A. Baker, Jr., Essentials of Padé Approximants (Academic Press, New York, 1975).
- <sup>11</sup> H.E. Stanley, Introduction to Phase Transitions and Critical Phenomena (Oxford Univ. Press, New York, 1971).

- <sup>12</sup>P. Steinhardt, Phys. Rev. D16, 1782 (1977).
- <sup>13</sup>J. Kogut, lectures presented at the International Summer School, McGill University (1976).
- <sup>14</sup>A. Zee, Phys. Rev. D12, 3251 (1975).
- <sup>15</sup>H. Bergknoff, Nucl. Phys. B122, 215 (1977).
- <sup>16</sup>G. Frye, R. Fredrickson, unpublished.

#### FIGURE CAPTIONS

- Fig. 3.1: The lattice.
- Fig. 4.1: The diagram distinguishing the two vacua.
- Fig. 5.1: The action of  $H_h$ .
- Fig. 5.2: A graph requiring the  $\rho \cdot \rho$  term.
- Fig. 6.1: The binding energy of the Schwinger model. The lower curve is obtained from an approximate continuum calculation, while the upper curve is a lattice calculation.
- Fig. 7.1: Two second order vacuum diagrams.
- Fig. 7.2: A third order graph. Note that the vacuum fluctuation consists here of heavy quarks.
- Fig. 7.3: A fourth order graph.
- Fig. 7.4: Three of the 9 fourth order graphs involving  $H_\Delta^2$ .
- Fig. 11.1: Third order contributions to a particle mass.
- Fig. 11.2: Some 4th order particle graphs.
- Fig. 11.3: A fourth order particle graph involving  $H_\Delta^2$ .
- Fig. 12.1: Pade's of mass ratios.
- Fig. 12.2: Dependence of mass ratios on the variable RL.
- Fig. 12.3: Dependence of  $M_\pm$  on  $\underline{RH}$ .

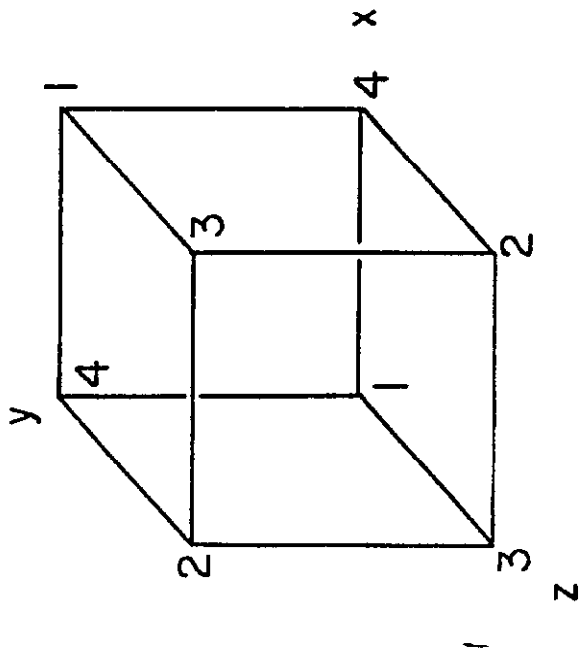


Fig. 3.1

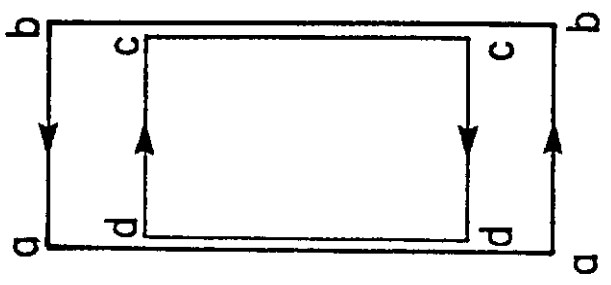


Fig. 4.1

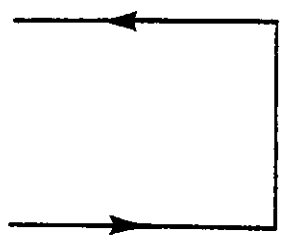


Fig. 5.1



Fig. 5.2

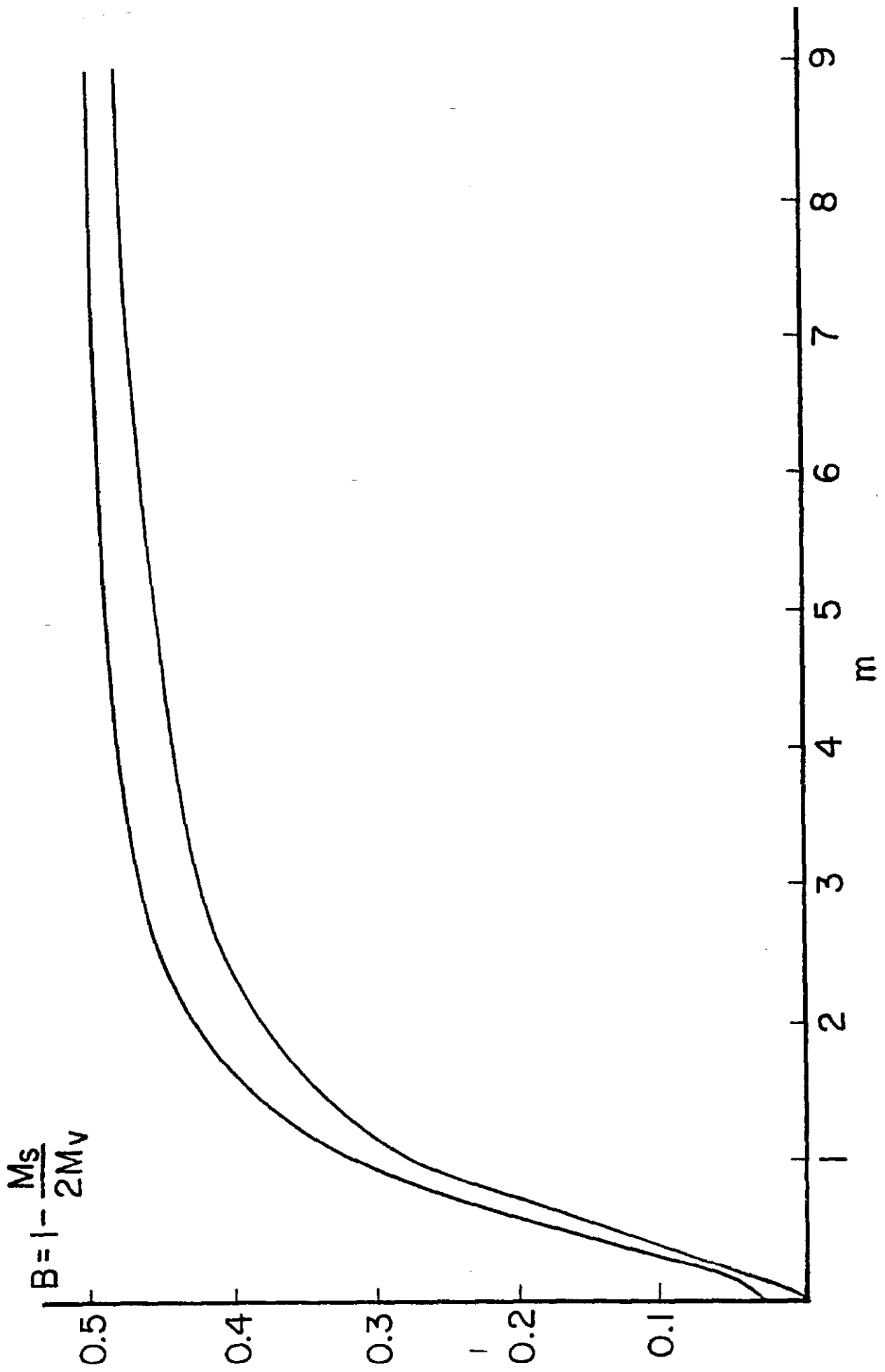


Fig. 6.1

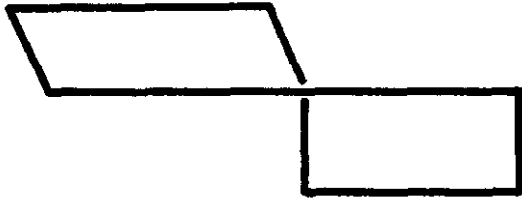


Fig. 7.2

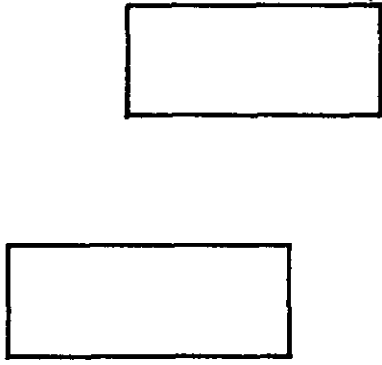


Fig. 7.3



Fig. 7.1



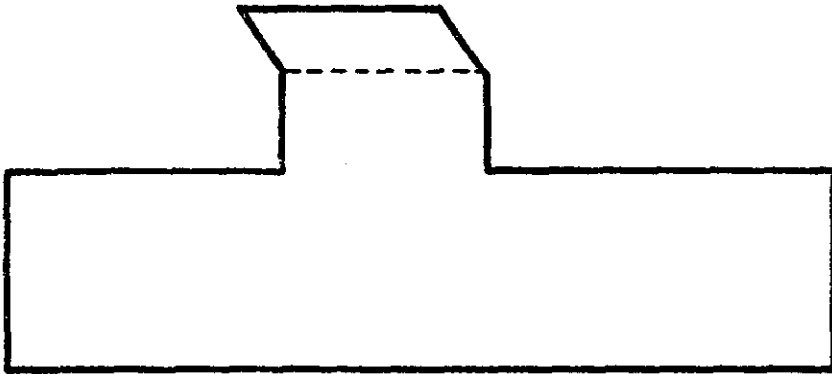
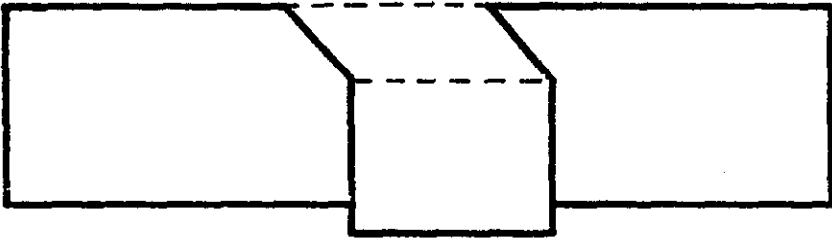
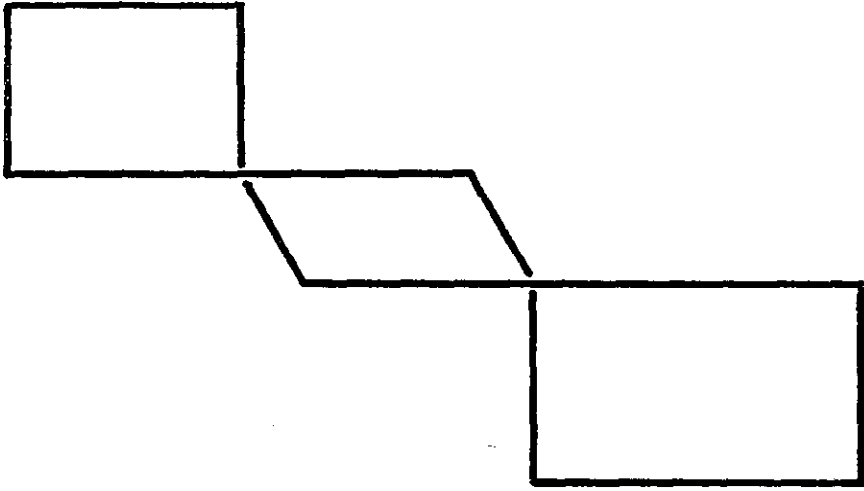


Fig. 7.4

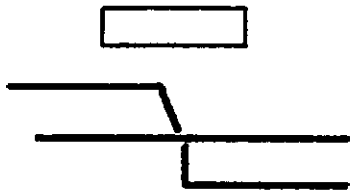
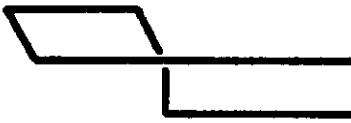
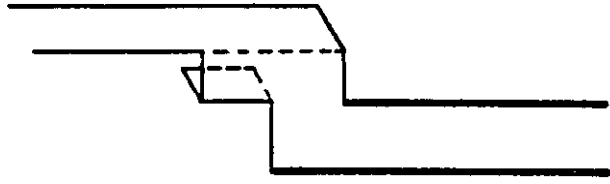


Fig. 11.1

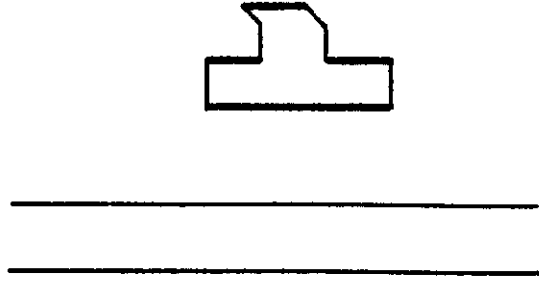


Fig. 11.3

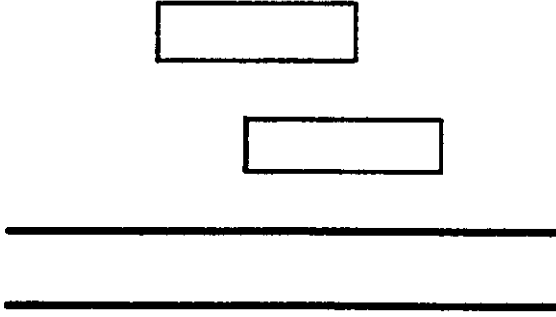
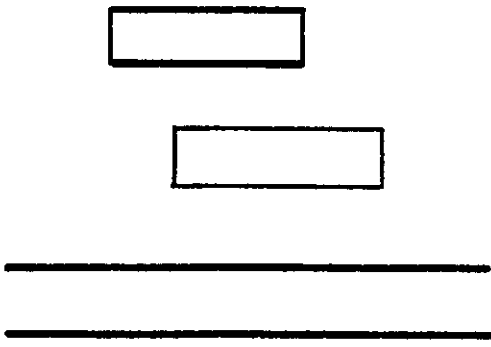


Fig. 11.2



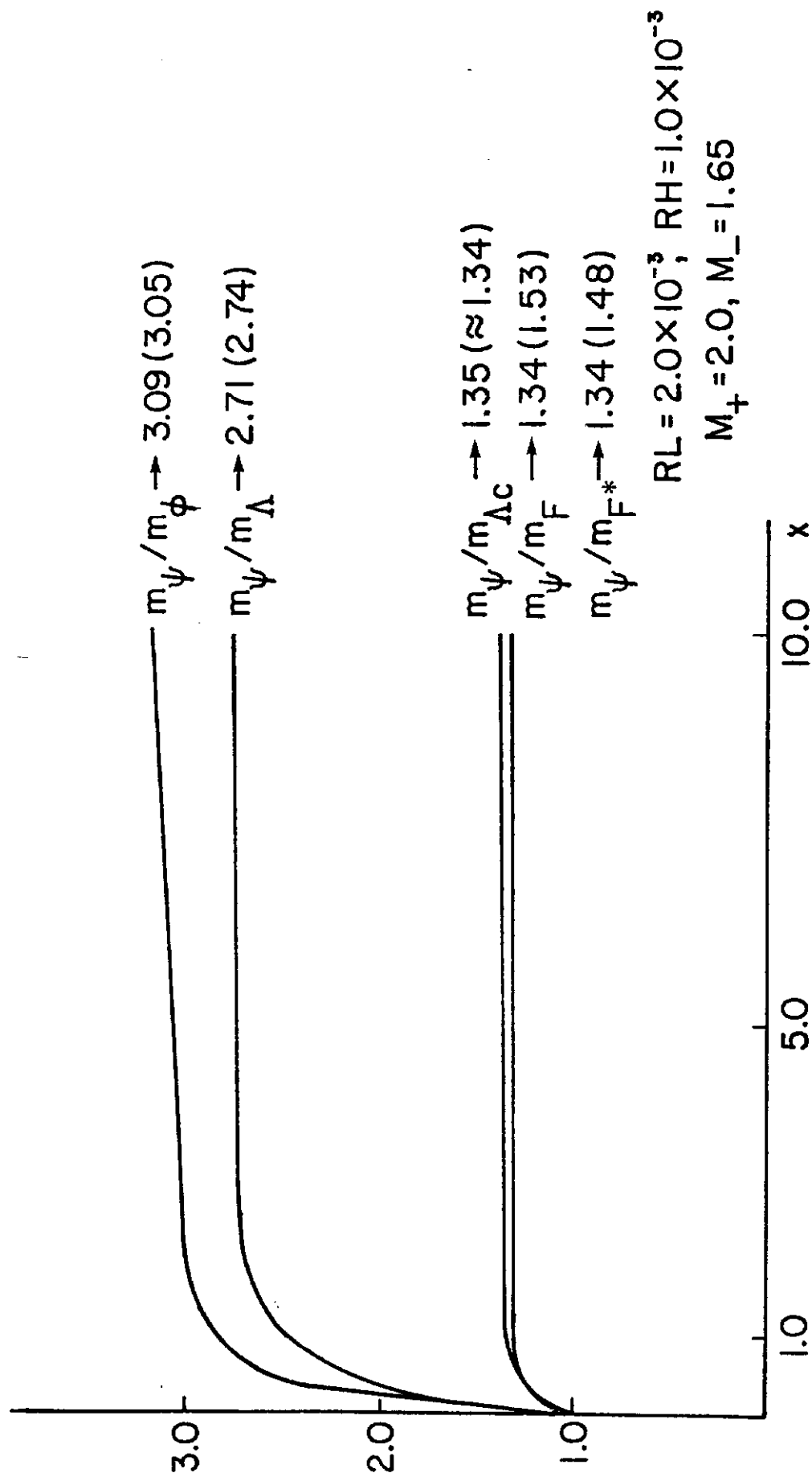


Fig. 12.1

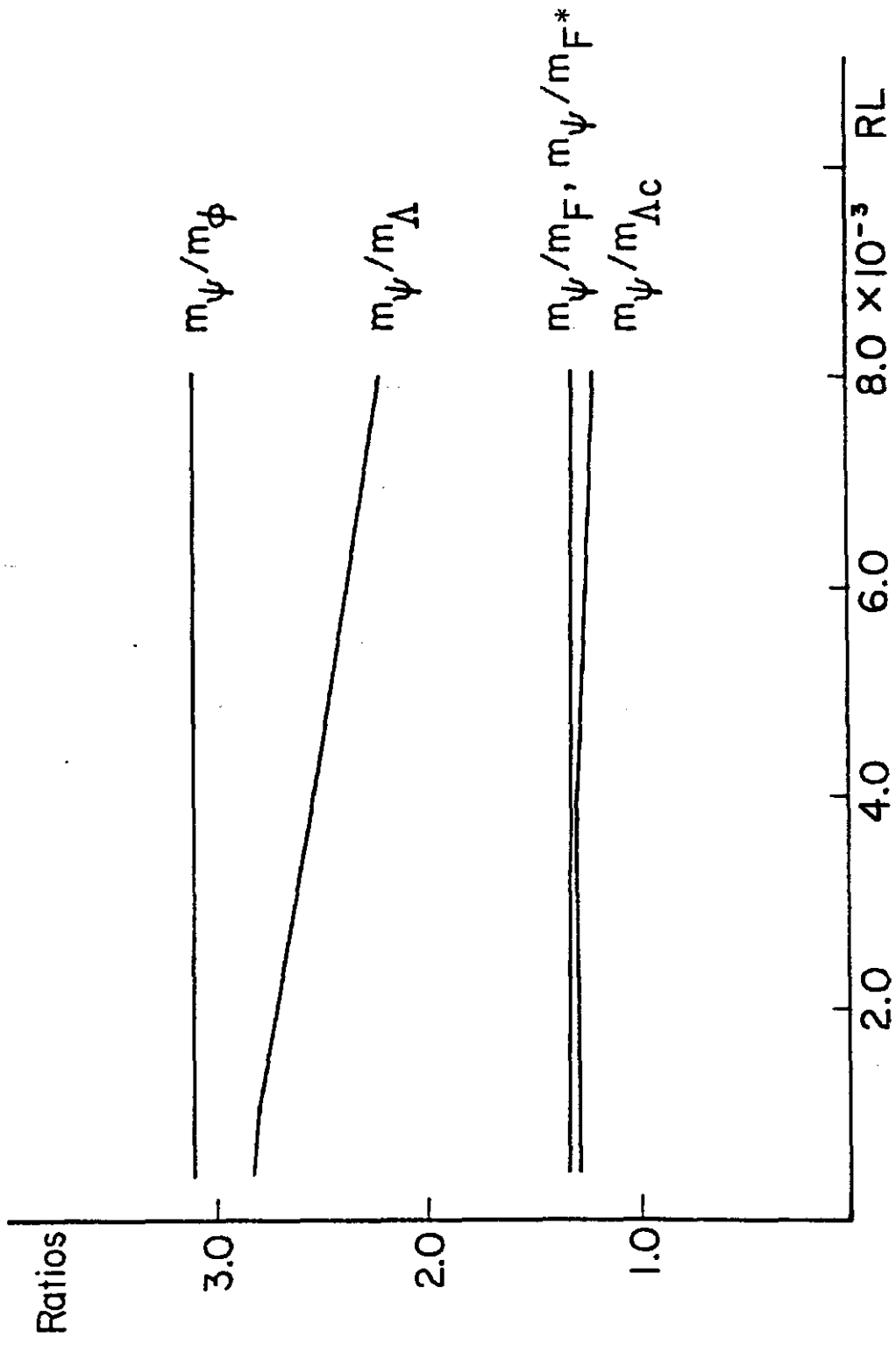
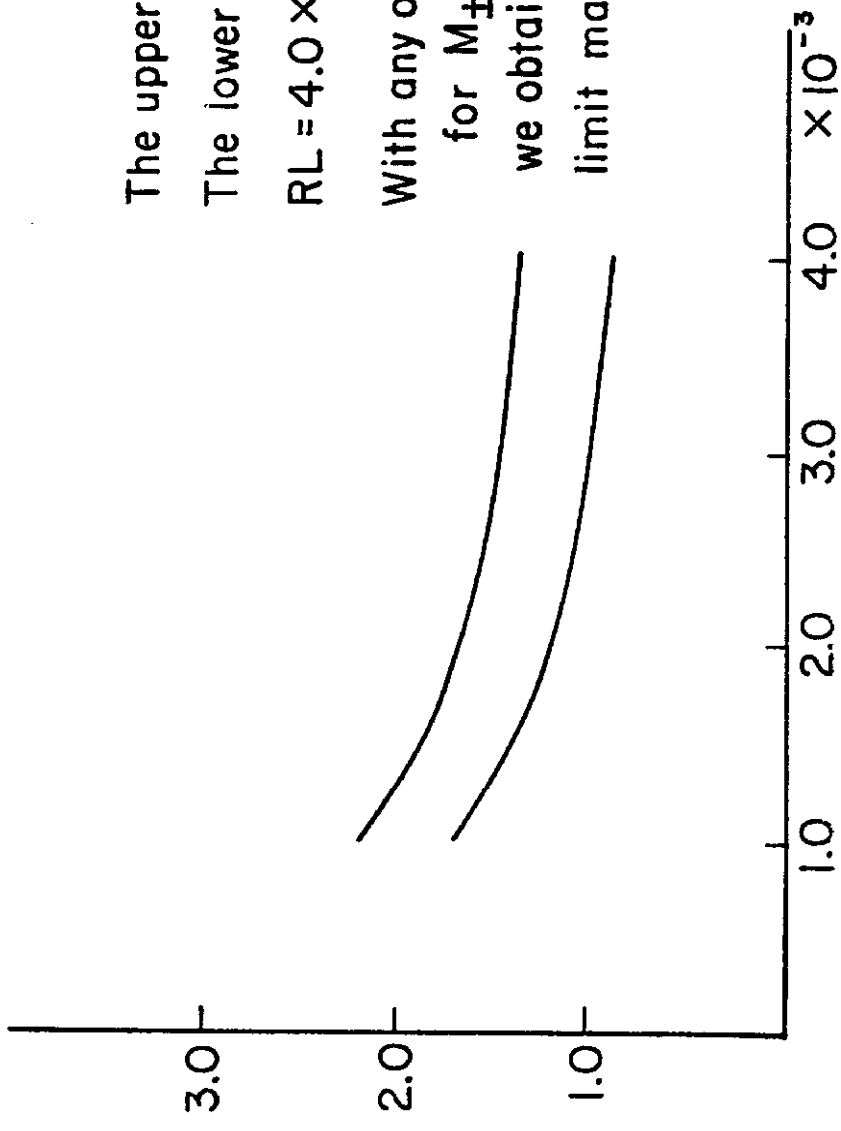


Fig. 12.2



The upper curve is  $M_+$

The lower curve is  $M_-$

$RL = 4.0 \times 10^{-3}$  is fixed

With any of these values

for  $M_{\pm}$ ,  $RL$ ,  $RH$

we obtain the same continuum

limit mass ratios for our particles

Fig. 12.3